



Full paper



Low-power, deformable, dynamic multicolor electrochromic skin

Jehyoung Koo^{a,1}, Vipin Amoli^{a,1}, So Young Kim^a, Chaeyoung Lee^a, Junho Kim^b,
Sung-Min Park^{b,c}, Jeongsun Kim^d, Joon Mo Ahn^d, Kyung Jin Jung^d, **Do Hwan Kim^{a,e,*}**

^a Department of Chemical Engineering, Hanyang University, Seoul, 04763, South Korea

^b School of Interdisciplinary Bioscience and Bioengineering, Pohang University of Science and Technology, Pohang, 37673, South Korea

^c Department of Creative IT Engineering, Pohang University of Science and Technology, Pohang, 37673, South Korea

^d Agency for Defense Development, Daejeon, 34186, South Korea

^e Institute of Nano Science and Technology, Hanyang University, Seoul, 04763, South Korea

ARTICLE INFO

Keywords:

Low-power
Dynamic multicolor electrochromic skin
Deformable
Iontronic polymer pump
Active camouflage

ABSTRACT

Active camouflage exhibited by certain creatures in nature such as cephalopods has inspired the fabrication of display devices for human-adaptive camouflage technologies. In order to realize that, electrochromic devices (ECDs) have attracted significant attention owing to their low-voltage operations and fast responses. However, the effective utilization of ECDs requires multicolor patterning, durable functioning, and wearable characteristics, simultaneously, but has not been explored. Here, we demonstrate a low-power, deformable, dynamic multicolor electrochromic skin (DMECS) that mimics the multicolor patterning and the active camouflage functionalities of the skins of cephalopods. The electrochromic polymers such as poly(3-hexylthiophene-2,5-diyl), poly[2-methoxy-5-(2-ethylhexyl-oxy)-1,4-phenylenevinylene], and P4a (green color polymer) are used to create purple, orange, and green colors, respectively. An iontronic polymer pump composed of an ionic liquid (1-ethyl-3-methylimidazolium bis(trifluoromethylsulfonyl)imide) incorporated in thermoplastic polyurethane is used as a deformable and transparent solid-state electrolyte that enables low-voltage (± 3 V) operated DMECS with excellent cyclic coloration/bleaching stability ($>35,000$ s), fast response (~ 1.75 s), and high durability under repeated 10,000 cycles of compressive force (with a bending radius of 8 mm) and tensile strains ($\sim 100\%$ up to 15,000 s). We believe that our DMECS can offer user-controlled selective coloration/bleaching of arbitrary display patterns and open new avenues for next-generation wearable optoelectronics.

1. Introduction

As active multicolor changing systems, the skins of certain natural creatures such as cephalopods (cuttlefish, octopus, and squids) have inspired researchers to design more conformable and intelligent devices for futuristic adaptive camouflage technologies including military adaptive camouflage and multicolor wearable displays [1–5]. Over the past few decades, various wearable emissive and non-emissive displays have been developed, which are expected to provide new opportunities in wearable displays and camouflage devices. In general, emissive displays exhibit the advantages of high color purities and fast responses, but it is difficult to observe their emissive abilities under sunlight [6–10]. On the other hand, non-emissive displays based on chromic phenomena such as mechanochromism [5,11], thermochromism [12,13], photochromism [14], and electrochromism [15] not only

demonstrate feasibility even under sunlight but also the advantage of simple device fabrication. In contrast to other chromic devices, whose display characteristics are mainly governed by the external stimuli (e.g. mechanical stress, temperature, and light) and difficult to control, electrochromic devices (ECDs), which change their colors reversibly under an applied voltage, have demonstrated user-controlled functions [16,17]. A typical ECD consists of an electrolyte layer sandwiched between an electrochromic active material deposited on a transparent electrode. The color change in the electrochromic active material occurs upon electrochemical redox reactions owing to the injection/extraction of electrons and ions from the electrode and electrolyte, respectively [18–21].

Various electrochromic materials including metal oxides [22], viologens [23], and electrochromic polymers [24] (ECPs) have been extensively investigated. Among them, ECPs have attracted considerable

* Corresponding author.

E-mail address: dhkim76@hanyang.ac.kr (D.H. Kim).

¹ These authors contributed equally to this work.

interest owing to their high coloration efficiencies, high contrast ratios, and simple color tunability through molecular design [25–27]. Despite the significant progress in ECDs, the realization of ECDs in adaptive camouflage technologies further demands multicolor patterning, durable functioning, and wearable characteristics (i.e., maintenance of good performance under physical deformations as well as adaptability in real life environments comprising complex bending and strains), which is rather difficult to achieve for conventional liquid electrolyte-based ECDs. Recently, the use of mechanically robust ion gels in ECDs has led to the fabrication of flexible and durable ECDs for next-generation wearable display applications [28,29]. However, the trade-off relationship between the ionic conductivity and mechanical properties requires a sensible selection of gel composition [30,31]. Therefore, in order to apply ECDs in adaptive camouflage technologies, it is essential to resolve these issues [32,33].

Here, inspired from the multicolor patterning and active camouflage

functionalities of cuttlefish skin, we demonstrate a low-power, deformable, dynamic multicolor electrochromic skin (DMECS) through the integration of multicolor flexible ECDs and silicon integrated circuits that are consolidated on a printed circuit board (PCB). A deformable DMECS is fabricated using poly(3-hexylthiophene-2,5-diyl) (P3HT), poly[2-methoxy-5-(2-ethylhexyloxy)-1,4-phenylene-vinylene] (MEH-PPV), and P4a (green color polymer) [34] as ECPs and ionic thermoplastic polyurethane (i-TPU) incorporated by ionic liquid (IL), 1-ethyl-3-methylimidazolium bis(trifluoromethylsulfonyl)imide ([EMIM]⁺[TFSI][−]) as an iontronic polymer pump that serves as a solid-state electrolyte [35]. The fabricated DMECS demonstrates low-voltage operation (± 3 V), excellent coloration/bleaching stabilities ($>35,000$ s), fast switching times (~ 1.75 s/1.5 s), and even remarkable durabilities even after 10,000 cycles of repetitive mechanical bending (with a bending radius of 8 mm) and tensile strain tests ($\sim 100\%$ up to 15,000 s). We utilized the advantage of the versatility of the i-TPU towards a wide range of ECPs (P3HT,

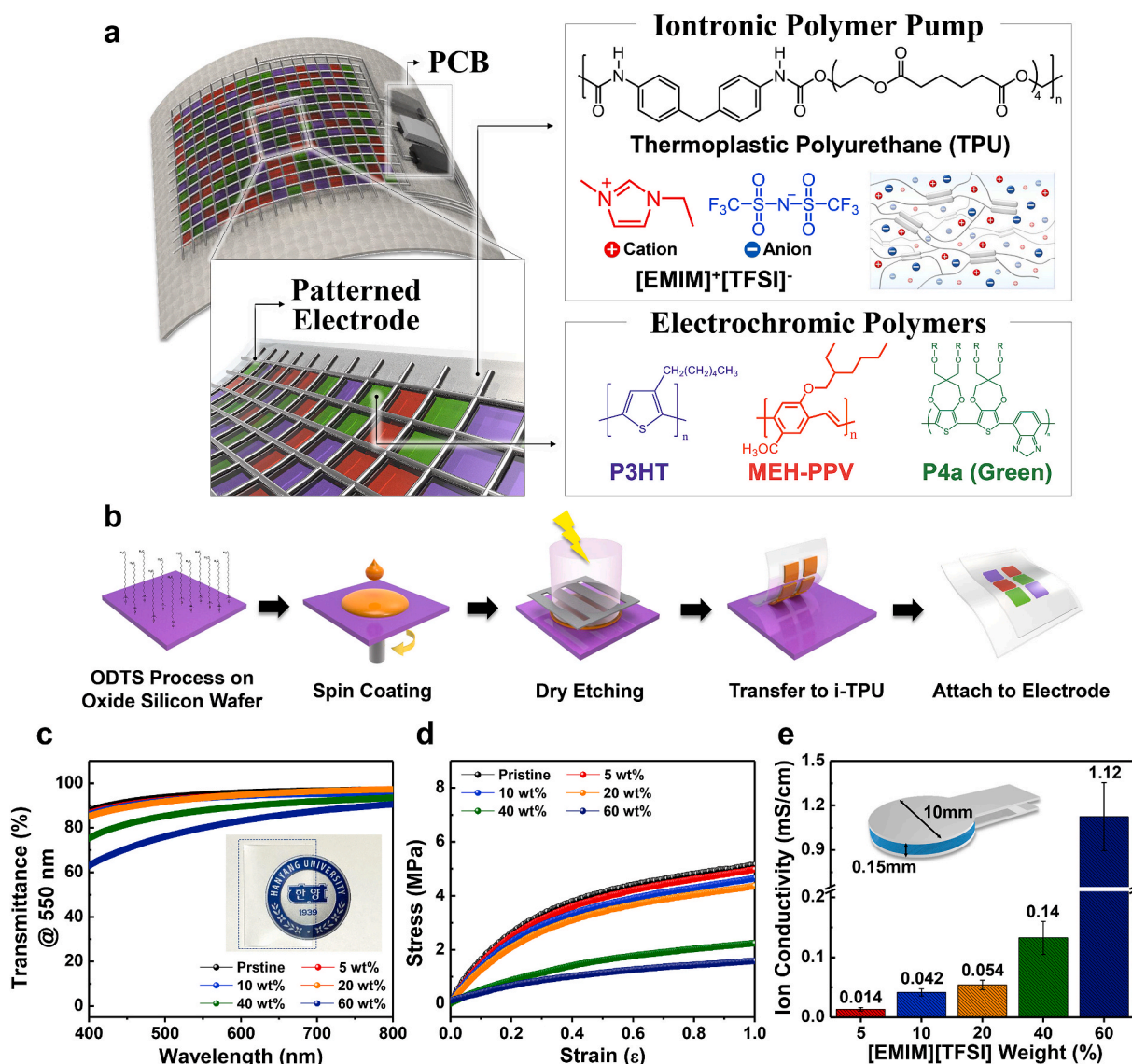


Fig. 1. Design of low-power, deformable DMECS. (a) Schematic of our DMECS and the chemical structures of its associated components. P3HT, MEH-PPV, and P4a ECPs were used to create purple, orange, and green colors, respectively while i-TPU ([EMIM]⁺[TFSI][−] loaded in TPU polymer chains) was used as a highly flexible solid-state electrolyte. The DMECS was fabricated by sandwiching a multicolor pattern-ECP incorporated i-TPU film between two flexible electrodes. (b) Schematic illustration of the fabrication procedure of multicolor pattern-ECP incorporated i-TPU films in our work. (c) Transmittance spectra of i-TPU films (0–60 wt% of IL) at 550 nm. Inset shows photo of i-TPU placed on HANYANG UNIVERSITY logo, indicating high transparency. (d) Stress–strain curves of i-TPU films (0–60 wt% of IL). (e) Ion conductivities of i-TPU films (0–60 wt% of IL). Inset shows electrode/i-TPU/electrode cell structure used in EIS experiments. (For interpretation of the references to color in this figure legend, the reader is referred to the Web version of this article.)

MEH-PPV, and P4a in our case) to fabricate a highly flexible DMECS that directly mimics the skin patterns of the cuttlefish. Potentially, our DMECS offers user-controlled selective coloration/bleaching of arbitrary display patterns, similar to active camouflage ability of cuttlefish, and hence opens new avenues for futuristic adaptive camouflage technologies.

2. Results & discussion

Fig. 1a shows a schematic of deformable DMECS and chemical structures of its associated components. P3HT, MEH-PPV, and P4a were used to create purple, orange, and green colors, respectively while the i-TPU was used as a highly flexible solid-state electrolyte. The DMECS was fabricated with an interlayer structure that shows a multicolor pattern-ECP film incorporated i-TPU as an active layer sandwiched between two flexible electrodes (indium tin oxide (ITO)-polyethylene terephthalate (PET) and patterned Cr/Au-PET electrodes; for details, see [Experimental section](#)). By utilizing mechanically flexible components (i.e., multicolor ECP film-incorporated i-TPU flexible active film and flexible PET substrates), a highly flexible or wearable DMECS was fabricated, while the PCB technology was utilized to incorporate wireless-assisted, user-controlled functionalities for adaptive camouflage (will be discussed later in detail). As illustrated in Fig. 1b, a simple transfer technique was utilized for the incorporation of patterned ECP films on the i-TPU. In the first step, ECPs films (thickness: ~80 nm) were fabricated on self-assembled monolayer (SAM) substrates (octadecyltrichlorosilane (ODTS)-treated n-doped Si/SiO₂ wafer) through spin-coating process. Subsequently, a dry etching process was carried out to create patterns having controlled shapes, sizes, and inter-distances (Fig. S1). For the transfer process, the i-TPU was cut into desired dimensions and applied to the ECP patterns on the SAMs substrates, and subsequently smoothed down with a finger. The visco-poroelastic nature of the i-TPU enabled an intimate interface with the SAMs substrate and facilitated the transfer of the ECP patterns on the i-TPU during peel-off process [35].

The i-TPU was fabricated through the non-covalent interactions of [EMIM]⁺[TFSI]⁻ pairs in the TPU matrix (see [Experimental section](#)), which served as a mechanically robust, highly transparent solid-state electrolyte. As reported, the important requirements of ionic polymers for applications in flexible ECDs are (i) optical transparency, (ii) mechanical robustness, and (iii) ionic conductivity [36]. To fabricate an optimal i-TPU with the best combination of optical, mechanical properties, and ionic conductivity, we fabricated and characterized a series of the i-TPU (0–60 wt% of IL). Fig. 1c shows the transmittance spectra of the i-TPU (thickness: ~150 μm). The i-TPU (0–60 wt% IL) exhibited high transparencies but the transmittance decreased with an increase of IL content (Table S1). For lower IL contents i.e., up to 20 wt% (20i-TPU), the high transmittance was almost maintained (a marginal decrease of ~1.4%, compared to pristine TPU), compared to the i-TPU films with 40 and 60 wt%. Similarly, the mechanical properties of the i-TPU were largely affected by the IL content. The representative stress-strain curves of the i-TPU (0–60 wt% IL) are shown in Fig. 1d. A decrease in Young's modulus (Table S2) with an increase of IL content can be attributed to the plasticizing effect of the ions in the TPU chains [35]. In particular, a relatively high Young's modulus was maintained up to 20 wt%, but beyond this value the modulus significantly decreased.

Similar to the optical and mechanical properties, the ionic conductivity of the i-TPU could be significantly tuned by the IL content. Fig. 1e shows the ionic conductivity of the i-TPU as a function of the IL content (0–60 wt%), evaluated by electrochemical impedance spectroscopy (EIS) measurements (see [Experimental section](#)). As mentioned in previous reports, the high ionic conductivity results in low-voltage operation and fast switching of the ECDs [36]. The ionic conductivities signify that the 60i-TPU should be promising for use in ECDs. However, at IL concentrations beyond 20 wt%, the optical and mechanical properties were significantly weakened, as discussed (Fig. 1c and d). Furthermore, owing to the more fluidic nature of the i-TPU at a high concentration of the IL (particularly at 60 wt%), the IL leakage issues from 60i-TPU

became dominant, which is detrimental to the stability of the ECDs [29]. The optical, mechanical, and electrical investigations of the i-TPU reflect that for low IL contents (i.e. 5 and 10 wt%) excellent optical and mechanical properties but poor ionic conductivities are obtained, whereas for high IL contents (i.e. 40 and 60 wt%), excellent ionic conductivities but poor optical and mechanical properties are obtained. Therefore, we utilized 20i-TPU owing to its excellent transparency, high mechanical robustness, and prominent ionic conductivity for the fabrication of the DMECS. Prior to the fabrication of the DMECS, each ECD was fabricated separately by using P3HT, MEH-PPV, and P4a as ECPs, 20i-TPU as the solid electrolyte, and ITO-PET (~120 μm) as a flexible electrode. The ECDs were fabricated by sandwiching ECP (P3HT, MEH-PPV, and P4a)-film-incorporated 20i-TPU active film between two ITO-PET flexible electrodes.

Fig. 2a–c shows the representative absorption spectra of the P3HT, MEH-PPV, and P4a ECDs in the visible range at different applied biases. Notably, the broad absorption maximum observed for each ECD at 0 V, largely decreased at a bias voltage of +3 V and the devices exhibited fully bleached states. Upon the reversal of the polarity of the applied bias (−3 V), the absorption spectra perfectly regained their original shapes and the devices exhibited coloration states even different pixel sizes (Fig. 2a–c, insets, Fig. S2 and Supplementary movies B.1–B.3). When applied bias is OFF (i.e., 0 V), However, the device does not return to its initial state (i.e., P3HT film does not regain its original color). As shown in Fig. S3, the optical transmittance of the P3HT film is not restored when the bias voltage is turned OFF. In order to maintain its initial state (coloration state), we need to apply −3 V. Therefore, in experimental conditions, a constant voltage must be applied continuously in order to maintain the bleaching state.

For example, the bleached and colored states in the P3HT were reflected in the changes in color, purple (0 V) → pale blue (+3 V) → purple (−3 V). The formation mechanism of bleaching/coloration states in the various ECDs (Fig. 2d) can be explained as follows: At a positive bias voltage (+3 V) applied on the bottom electrode (Fig. 2d(ii)), electrons are extracted from P3HT and flow to the ITO, while the [TFSI]⁻ ions are pumped from the i-TPU to the P3HT layer to maintain charge neutrality. This creates $n[\text{P3HT}]^+m[\text{TFSI}]^-$ and finally leads to the oxidation of the P3HT film. In this process, the film becomes pale blue (bleached state) and the optical absorption largely decreases. On the other hand, when a negative bias voltage (−3 V) is applied to the bottom electrode, electrons are injected while [TFSI]⁻ are extracted from the $n[\text{P3HT}]^+m[\text{TFSI}]^-$ host (Fig. 2d(iii)). This reduces the $n[\text{P3HT}]^+m[\text{TFSI}]^-$ content and restores P3HT. In this process, the film becomes purple (coloration state) and the optical absorption is restored. Similar electrochemical doping of P3HT with various ions including [TFSI]⁻, [PF₆]⁻, [ClO₄]⁻, and Li⁺ have been reported [18–21]. The redox reactions in the P3HT ECD under our experimental conditions can be expressed as follows:

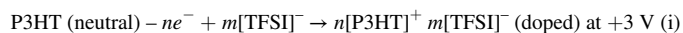


Fig. S4 represents the schematic of chemical structure of P3HT in neutral and doped state. Upon doping the chemical structure of neutral P3HT changes from benzoid-like to quinoid-like structure due to the formation of positive charge on the polymer chains [37]. Polarons and bipolarons are formed as different states of positive charge carriers along the P3HT polymer backbone due to the electrochemical doping of P3HT. The change in electronic structure of the P3HT as a result of electrochemical oxidation or reduction (as shown in equation (i) & (ii)) shifts the π - π^* electronic absorption resulting in the color change. To support our hypothesis of electrochemical doping in the P3HT, MEH-PPV, and P4a under the external applied bias, we monitored the ultraviolet–visible–near infrared (UV–vis–NIR) absorption spectra of the various ECDs in the potential range of 0.5–2.0 V. As shown in Fig. 3a, for the P3HT ECD, the absorption band (400–630 nm) related to the optical band gap of P3HT continuously decreased with the increase in the

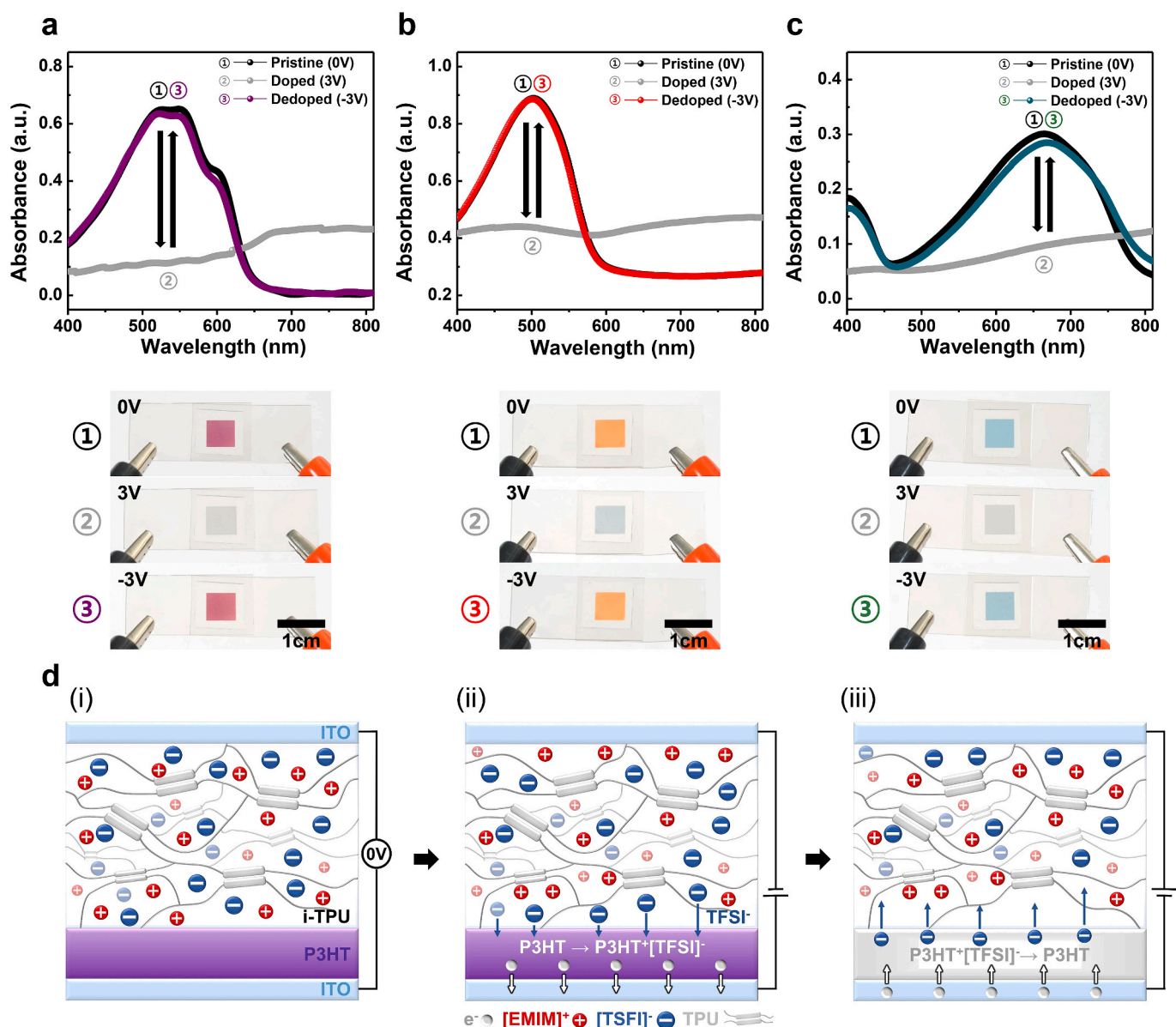


Fig. 2. Optical characterization and working principle of ECDs. UV-vis absorption spectra of (a) P3HT, (b) MEH-PPV, and (c) P4a ECDs with different applied voltages. Insets show photographs of the ECDs in colored, bleached and recolored states. (d) Schematic illustration of the working mechanism in i-TPU based ECDs (for descriptive purposes only P3HT is represented).

applied voltage. The two new bands in NIR range (characteristics of polaron and bipolaron states in P3HT) emerged in the ranges of 630–1000 and 1100–2400 nm and continued to increase up to 2 V. The observed spectral changes of the P3HT under the different applied voltages can be explained by the schematic of energy level diagram in Fig. 3b. The absorption band of P3HT (Fig. 3a) at 400–630 nm originated from the electronic transition from the highest occupied molecular orbital (HOMO) to the lowest unoccupied molecular orbital (LUMO) and corresponds to the optical band gap of neutral P3HT (*cal.* 1.85 eV). Polarons and bipolarons were formed once P3HT was doped upon extraction of electrons and the pumping of [TFSI]⁻ anions from the i-TPU. Regarding the polaron, two localized electronic states, $+\epsilon_0$ and $-\epsilon_0$ levels were generated in the band gap of the neutral P3HT. Therefore, the observed NIR absorption band at 630–1000 nm can be assigned to the polaron state transition P_2 from the $+\epsilon_0$ level to the $-\epsilon_0$ level, while the observed NIR absorption band at 1100–2400 nm can be assigned to polaron state transition P_1 (Fig. 3b(ii)). At high doping levels of P3HT, the formation of bipolarons was expected and two new localized

electronic states ($+\epsilon_0'$ and $-\epsilon_0'$ levels) deeper than the corresponding polaron state (ϵ_0) were generated. Therefore, some of the transitions in the NIR absorption bands can be assigned to the transition BP_1 of the bipolaron (Fig. 3b(iii)) [37–39].

Fig. 3c shows a cyclic voltammogram (CV) of the P3HT ECD in the potential range of ± 3.0 V. One oxidation peak (2.07 V) and one reduction peak (-2.36 V) were observed. The oxidation peak at 2.07 V indicates the oxidation of the P3HT (or p-type doping) to the polaron and bipolaron state, while the reduction peak at -2.36 V corresponds to the transition from the bipolaron and polaron to the neutral state. The other ECDs with MEH-PPV and P4a exhibited similar trends of absorption spectra under the different applied voltages (Fig. 3d and e). These spectroscopic investigations of the ECDs demonstrate the versatility of the i-TPU towards various ECPs, which encouraged us to fabricate the DMECS for adaptive camouflage.

In particular, long-term operational stability of each ECD is highly desirable for the fabrication of a reliable DMECS. Therefore, we investigated the coloration/bleaching cyclic stabilities of the ECDs based on

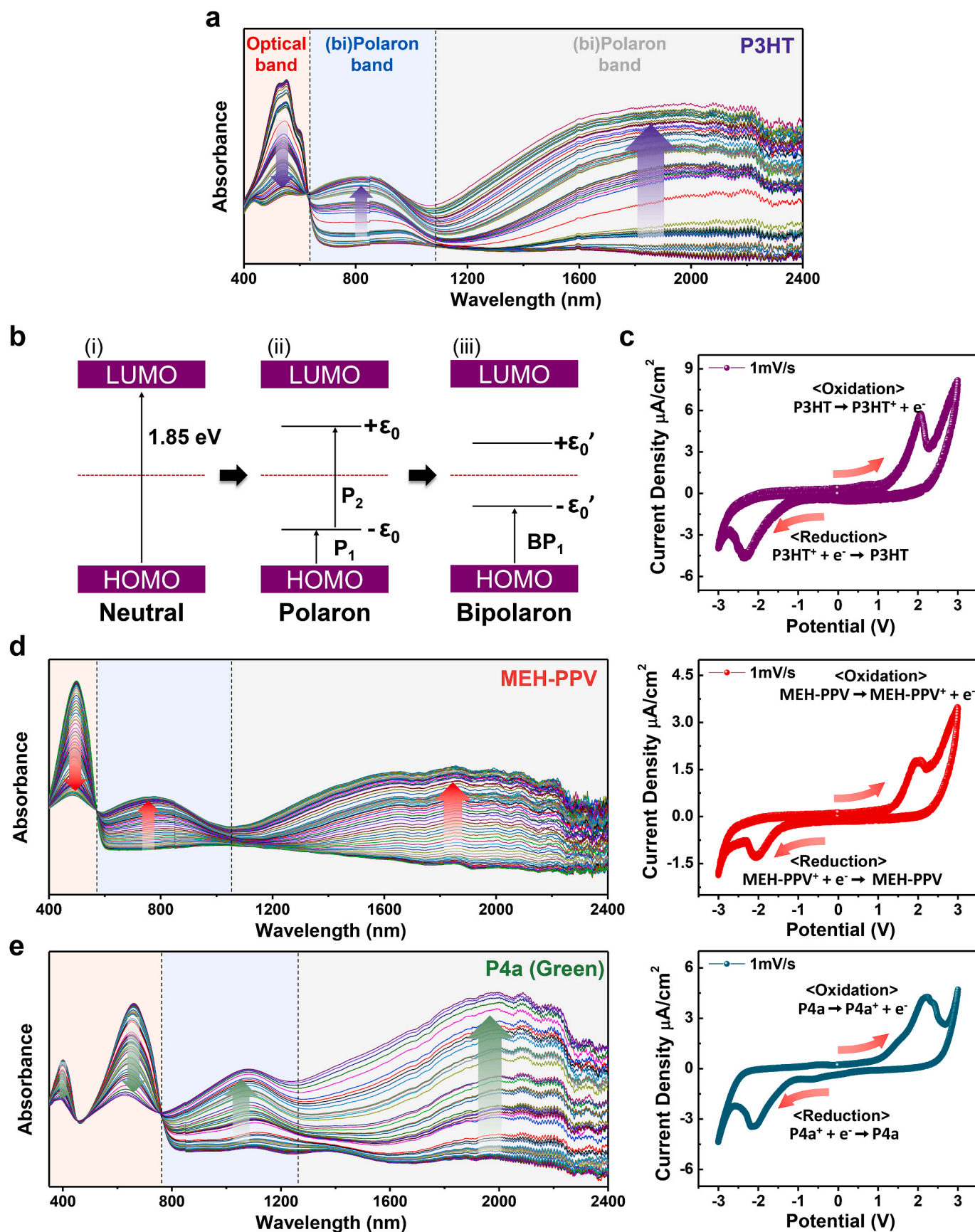


Fig. 3. Electrochemical doping mechanism of ECPs. (a) UV-vis-NIR absorption spectra of P3HT ECD in the potential range of 0.5–2.0 V. (b) Schematic illustration of energy-level diagrams of neutral, polaron and bipolaron states in P3HT. (c) CV of P3HT ECD. (d), (e) UV-vis-NIR absorption spectra of MEH-PPV and P4a ECD in the potential range of 0.5–2.0 V. Insets show the corresponding CVs.

20i-TPU. Fig. 4a shows the transmittance of the P3HT ECD in the potential range of ± 3 V at 550 nm. Even after a continuous drive for 35,000 s, the P3HT ECD exhibited a highly stable response without significant degradation. The P3HT exhibited fast operation times (bleaching and coloration time of 1.75 s and 1.5 s, respectively (Fig. 4b) and excellent cyclic stability (Fig. 4c). The other ECDs fabricated with MEH-PPV and P4a also exhibited stable long-term cyclic behaviors (Fig. S5) with fast responses. In addition, Supplementary movie B.4 shows electrochromic effect of P3HT ECD in 95% humidity condition. Supplementary movie B.5 shows electrochromic effect of P3HT ECD at 80 °C. It is important to note that the P3HT ECD works well even high humidity and temperature. These results show the excellent stability and durability of each ECD based on the 20i-TPU. However, the fabrications of flexible or wearable ECDs demand excellent stabilities of the devices in complex environments (e.g. under external bending and stretching), while maintaining the electrochromic behaviors. To verify the sustainability of the i-TPU based ECDs in complex environments, a series of stretching and bending tests were performed. To verify the feasibility for stretchable applications, we fabricated ECDs with stretched films (ECP-incorporated i-TPU layers under strains of 50% and 100%) and recorded their optical transmittances at applied voltages of ± 3 V. We recorded the optical transmittances at different applied tensile strains and as a function of the number of bending cycles. As shown in Fig. 4d, the transient profiles of the ECDs fabricated with the P3HT-incorporated i-TPU layers in the 50% and 100% strained states were stable over 15,000 s, which confirms the excellent operational stability of the P3HT-incorporated i-TPU layers for stretchable device applications. For the bending test, the device was subjected to bending up to a radius of 8 mm, and then operated at a voltage of ± 3 V for 5 s alternately. As shown in Fig. 4e, a marginal change in T_{rec}/T_{neu} of $\sim 6.3\%$ (T_{rec} denotes the transmittance of the recoloring state, while T_{neu} denotes the transmittance of the neutral state at 550 nm) was observed for the P3HT even after 10,000 compressive bending cycles, which demonstrates the bending stability of the i-TPU based ECDs for flexible applications. The versatility of the i-TPU towards various ECPs for the fabrication of various ECDs with excellent long-term stabilities, bending/stretching durabilities, and low-voltage operations inspired us to fabricate a multicolor electrochromic skin mimicking the dynamic camouflage ability of cephalopods for adaptive camouflages.

The skin of the cephalopods, well disguised in the sea to match the surrounding objects (Fig. 5a), consists of chromatophore, iridophore, and leucophore [1,40]. In particular, the chromatophores are connected to each other in a network structure. The expansion and contraction of pigment cells by muscles determines the sizes of the pigments, which eventually yields an “on–off switch” behavior of the skin color (Fig. 5a, inset). Fig. 5b shows a photograph of the highly flexible large-area (8×8 pixels, size of each pixel ~ 0.25 cm²) DMECS attached to a model hand based on the on/off switch system of cephalopod’s pigments. As already discussed, a series of dry etching and transfer processes were carried out by using P3HT, MEH-PPV, and P4a ECPs to create purple, orange, and green colors, respectively in DMECS. Fig. S6 shows a schematic of the thermally evaporated Cr/Au-PET patterned electrode used to create selective and independent display patterns in large-area DMECS. As shown in Fig. 5c, the PCB delivered stable user-controlled functioning and wireless transmission characteristics by using easily available integrated circuit components. In brief, TPS22860DBVR is a dual-channel control, PCA9685PW 118 is 16-channel voltage controller, which ensured the independent control (on/off) of individual pixels in DMECS, and TPS62112RSAT and AP2112K-3.3TRG1MCP73831 are low-dropout linear regulator (LDO), which provided regulated output voltage. The circuit designs of various components are given Figs. S7 and S8. The multi-protocol system on chip (SoC) (nRF51822 Bluetooth 4.0 and ARM Cortex M0) facilitated the Bluetooth wireless data transmission from the mobile handset to the PCB for adaptive camouflage applications.

Fig. 5c inset (black box) illustrates the system-level functional block diagrams of hardware (H/W) components and custom-developed mobile

application. Fig. 5d illustrates the practical application of our DMECS for futuristic adaptive camouflage technologies including military adaptive camouflage and multicolor wearable displays, where the user wearing our DMECS is supposed to change its color in accordance with the surrounding objects through a Bluetooth-enabled mobile handset with a custom-developed application (FOND Color App, Supplementary movie B.6). The real-time photographs of DMECS over various backgrounds as shown in Fig. 5e clearly reflect the active camouflage ability of our DMECS. The selective coloration/bleaching patterns in DMECS in accordance to the background colors are obtained through a Bluetooth-enabled mobile handset with FOND Color App (Supplementary movie B.7). Furthermore, any arbitrary coloration/bleaching pattern can be stored and recalled by the user according to the change in background color. These results clearly establish the potential application of our DMECS for adaptive camouflage technologies.

3. Conclusions

In summary, we could implement a low-power, deformable DMECS showing various colors and realization of user-controlled selective coloration/bleaching of arbitrary patterns in DMECS, which directly mimicked the active camouflage functionalities of skin patterns of the cuttlefish. We utilized various ECPs (P3HT, MEH-PPV, and P4a) to create multicolor patterns through the transfer printing technique. The use of the i-TPU as a deformable and transparent solid-state electrolyte enabled low-voltage operation, fast switching, and excellent durability even under the compressive and tensile strains, which endowed excellent flexibility and stability to the DMECS. Compared to previous reports, DMECS developed in the presented work possesses prominent features. First, it is fabricated via a facile transfer technique and can be integrated over large areas. The multicolor features in DMECS directly mimic the multicolor patterning and active camouflage ability of cephalopods skins. Second, the use of a novel iontronic polymer pump composed of an ionic liquid incorporated in thermoplastic polyurethane chains as a highly deformable and transparent solid state electrolyte enabled low-power DMECS with excellent stability, fast response, and durability even under repeated cycles of mechanical stimuli deformations. Third, our DMECS offers user-controlled selective coloration/bleaching of arbitrary display patterns for potential application in futuristic adaptive camouflage technologies. We believe that our work opens new avenues for potential applications in human-adaptive camouflage and multicolor wearable displays.

4. Experimental section

4.1. Materials

Trichloroethylene (TCE), ODTS, toluene, chlorobenzene, chloroform and *N,N*-dimethylformamide (DMF) were purchased from Sigma-Aldrich, P3HT (M105) was purchased from Ossila, MEH-PPV and P4a were purchased from Nano Clean Tech, [EMIM]⁺[TFSI][−] was purchased from C-TRI, TPU beads (KA-480) were purchased from Kolon Industries, Inc., and poly(dimethylsiloxane) (PDMS; Sylgard 184) was purchased from Dow Corning Corporation. All materials were used as received without further purification.

4.2. Fabrication of 20i-TPU solid electrolyte film

TPU beads were dissolved in DMF in a mass ratio of 1:3 under continuous stirring at 80 °C for 30 min. Subsequently, 20 wt% of [EMIM]⁺[TFSI][−] with respect to the weight of the TPU was added into the solution for further stirring (80 °C, 14 h) to obtain a transparent 20i-TPU gel. In order to obtain a 20i-TPU of desired thickness, an optimized spin coating process was employed, where a thick PDMS film (5 mm) was used as the substrate. The PDMS substrate was formed by (i) curing a mixture of a base resin and crosslinker (mass ratio: 10:1) in a plastic

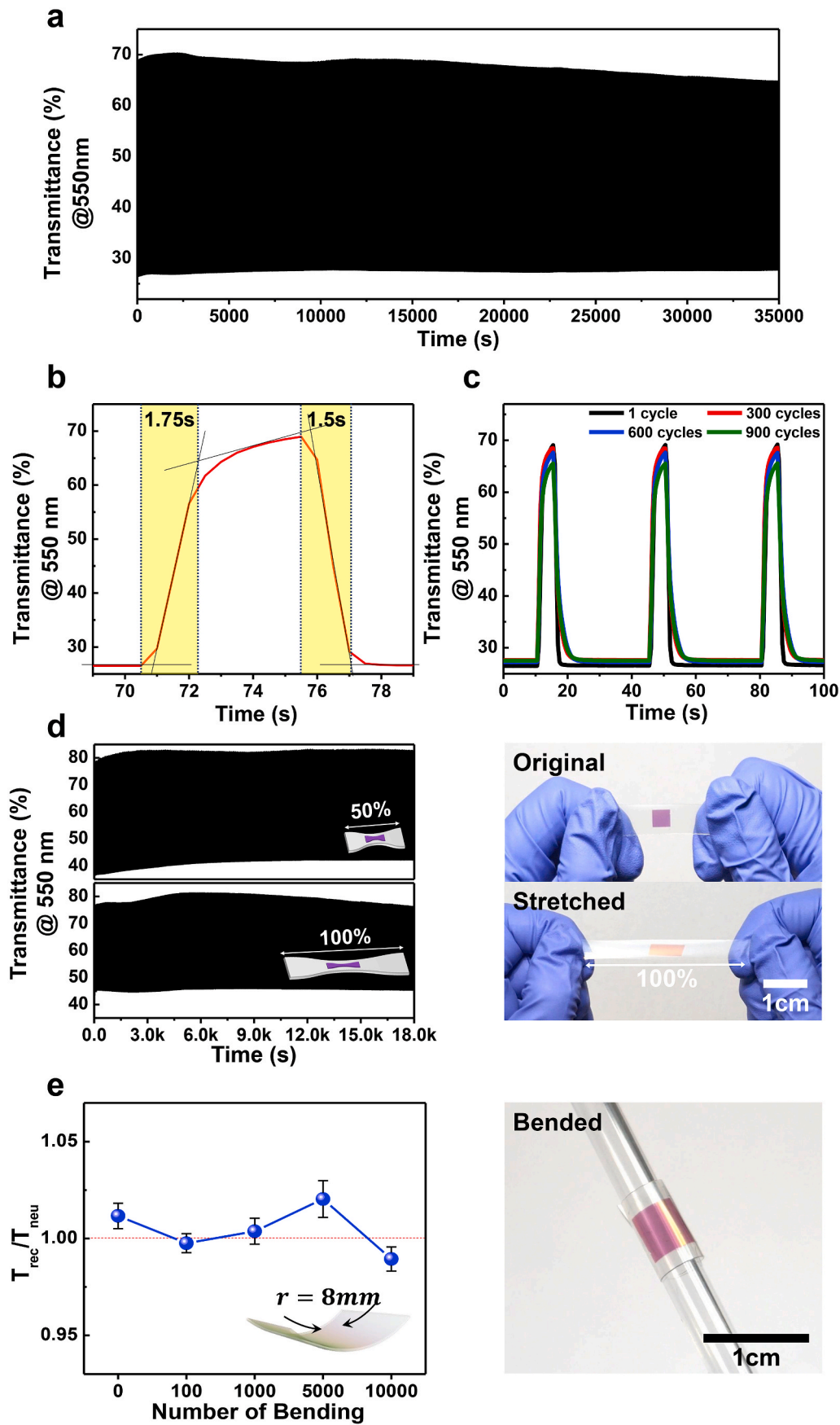


Fig. 4. Durability of ECD. (a) Transient transmittance profile at 550 nm during continuous coloration/bleaching switching cycles of the P3HT ECD. (b) Bleaching and coloration times. (c) Transient transmittance profile after 1, 300, 600, and 900 cycles of coloration/bleaching. (d) Transient transmittance profile of P3HT-incorporated i-TPU active layer in 50% and 100% stretched states. Inset right shows the photographs of P3HT-incorporated i-TPU film in normal and stretched states. (e) Changes in T_{rec}/T_{neu} in P3HT ECD as a function of number of bending cycles (bending radius ~ 8 mm). Inset right shows the photograph of flexible P3HT ECD wrapped around a glass pipette (radius ~ 2.5 mm).

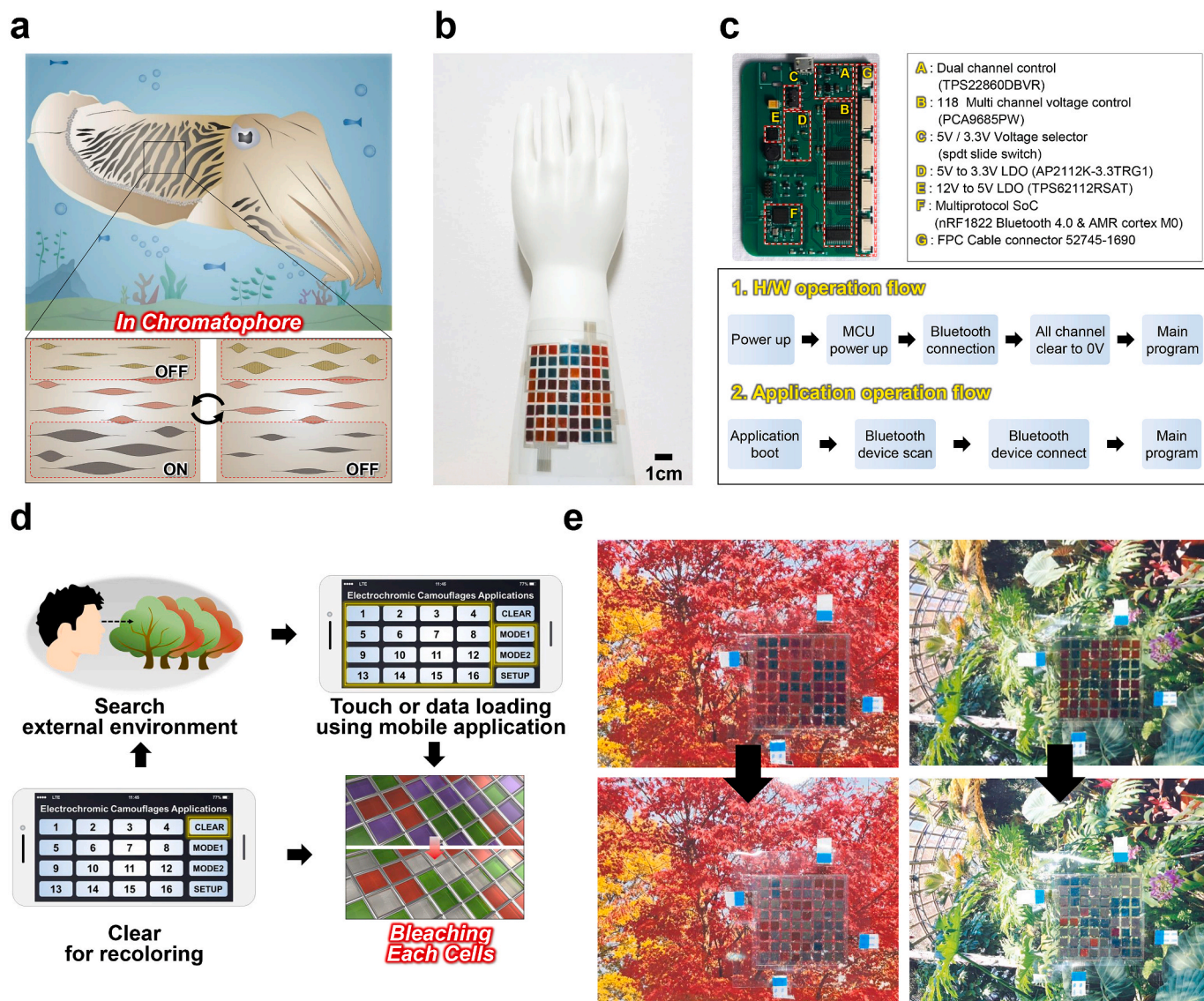


Fig. 5. Cephalopod-like DMECS for active camouflage applications. (a) A schematic of a cephalopod's skin. The colored regions are the pigment cells called 'chromatophores' that expand and contract in ON/OFF fashion to allow active camouflage. (b) Photograph of our low-power, deformable DMECS attached to a model hand. (c) Photograph of a commercially available PCB with different integrated circuit components labelling (right inset, silver box). Lower inset (black box) illustrates the system-level functional block diagrams of H/W components and custom-developed mobile application. (d) Schematic illustration of user-controlled active camouflage of DMECS. The user wearing our DMECS is supposed to change its color in accordance with the surrounding objects through a Bluetooth-enabled mobile handset with a custom-developed application (FOND color App). (e) Real-time photographs of DMECS over various backgrounds showing active camouflage for adaptive camouflage applications. (For interpretation of the references to color in this figure legend, the reader is referred to the Web version of this article.)

petri dish and (ii) degassing and curing in an oven at 80 °C for 2 h. Then 20i-TPU gel (15 g) was poured on the PDMS, spin-coated at 350 rpm for 90 s, and then heat-treated at 120 °C for 24 h (starting from 60 °C at a temperature ramp rate of 10 °C per hour) to fully remove the residual solvent under the optimized conditions and to obtain a transparent 20i-TPU (~150 μm). The other i-TPU films (5, 10, 40 and 60 wt%) were prepared under identical reaction conditions.

4.3. Fabrication of the ECP-film-incorporated i-TPU active films

ECP-film-incorporated i-TPU films (i.e., ECPs films on i-TPU) were fabricated by a three-step procedure involving (i) fabrication of ECPs films on SAMs substrate, (ii) patterning and then (iii) transfer to the i-TPU. In the first step, ECPs films were fabricated on SAMs substrates (ODTS-treated, heavily n-doped Si/SiO₂), and then transferred to i-TPU. To obtain SAMs substrate, n-doped Si/SiO₂ substrates (thickness = 3000

Å) were consecutively cleaned by sonication in acetone and isopropanol (for 15 min in each of them), and then surface-treated (PE, Femto Science) for 60 s. Subsequently, the cleaned substrates were dipped into a solution of TCE (20 mL) and ODTS (40 μL) at room temperature for 45 min, rinsed with toluene (to remove residuals), and then annealed at 145 °C for 30 min. The substrates were then wiped by a swab and cleaned by sonication in toluene for 10 min. For the fabrication of ECPs on SAMs substrate an optimized spin coating process was used. To obtain P3HT on SAMs substrate, a P3HT solution was prepared by dissolving P3HT in chlorobenzene (11 mg/mL) at 70 °C for 12 h under continuous stirring. Then the obtained solution was spin-coated on the SAMs substrate at 1000 rpm for 60 s and annealed at 180 °C for 3 h in nitrogen atmosphere to obtain the P3HT film on the SAMs substrate. Similar procedures were used for the fabrication of the other ECP films (MEH-PPV and P4a) on SAMs substrates. However, for the P4a polymer, chloroform was used as the solvent. In the second step, the ECP films on

the SAMs substrates were patterned through reactive-ion etching (Femtoscience) in an oxygen plasma atmosphere (30 sccm, 100 W, 0.05 torr) for 25 s. The dry etching process allowed the formation of ECPs patterns by controlling shapes, sizes and inter-distances without thickness decrease or polymer residues (Fig. S1). In the third step, in order to transfer ECPs patterns from SAM substrates to i-TPU, the 20i-TPU was cut into the desired dimensions and applied to the ECP films (P3HT, MEH-PPV, and P4a) on SAMs substrates heated at 80 °C for 60 s. Owing to the intimate interfacial contact between 20i-TPU and SAMs substrates, the ECP patterns (P3HT, MEH-PPV, and P4a) could be easily peeled off and transferred to the 20i-TPU.

4.4. Fabrication of flexible ECDs and large area DMECS

The ECP-incorporated 20i-TPU films (i.e., P3HT-incorporated 20i-TPU, MEH-PPV-incorporated 20i-TPU, and P4a-incorporated 20i-TPU) were sandwiched between two ITO-PET flexible electrodes (Nano Clean Tech) to fabricate a series of the ECDs with P3HT, MEH-PPV and P4a polymers. To fabricate the large-area DMECS (8 × 8 pixels, size of each pixel ~ 0.25 cm²), we utilized a multi-step reactive-ion etching and transfer process to create multiple colors (P3HT, MEH-PPV, and P4a ECPs to create purple, orange and green colors respectively) on SAMs substrate. A transfer process as described above was utilized to fabricate multicolor ECPs-film-incorporated 20i-TPU active film. The multicolor ECPs-film-incorporated 20i-TPU film was sandwiched between two flexible electrodes, i.e., an ITO-PET as the upper electrode and thermally evaporated patterned Cr (10 nm)/Au (40 nm)-PET (~25 μm) as the bottom electrode as shown in Fig. S6. Commercially available integrated circuit components (Figs. S7 and S8) consolidated on a PCB was used to incorporate user-controlled functioning. The DMECS was powered by three rechargeable lithium-ion batteries (3.7 V, 100 mA h) in series.

4.5. Design of custom mobile application

A mobile application FOND Color App (Supplementary movie B.6) was designed to provide user-controlled active camouflage display patterns in the DMECS developed in this study. To use this application, the user should open the Fond Color App on the mobile device. The application establishes a secure Bluetooth connection to the DMECS. The application could produce arbitrary and selective patterns through random and selective touches on the mobile. In addition, the bleaching/recoloring patterns could be stored on the device and recalled at any time.

4.6. Material characterization

A universal testing machine (UTM QRUTS-S105, QURO) with a 1-kN load cell was used for the mechanical testing of all i-TPU films at 25 °C with a stretching speed of 10 mm min⁻¹. Dumbbell-shaped specimens were fabricated and tested according to the American Society for Testing and Materials (ASTM) standard (Test Method D 638–02a, specimen type V). The Young's modulus (*Y*) was calculated by using the slope of the stress-strain curve (in the strain range of 0–5%). EIS measurements were performed at room temperature by using an electrochemical analyzer PGSTAT302 N (Metrohm Autolab) in a frequency range of 0.1 Hz–100 kHz with a 10-mV alternating-current signal. For the EIS measurements, i-TPU films (~150 μm) were sandwiched between two stainless-steel discs (diameter = 10 mm), used as electrodes. All impedance spectras were fitted by using the appropriate equivalent circuit models built in the NOVA software (Metrohm Autolab) to evaluate the bulk resistances (*R_b*) of the devices. The ionic conductivity was calculated by using *R_b* as $\sigma = l/(R_b \times A)$, where σ is the ionic conductivity, *l* is the thickness of the polymer film sandwiched between the electrodes, *A* is the area of the electrode, and *R_b* is the bulk resistance obtained by using the EIS Nyquist plot. The CVs of the ECPs were recorded by using a potentiostat (Metrohm Autolab) at a scan rate of 1 mV s⁻¹ in a two-electrode device

configuration (stainless-steel disc (electrode)/P3HT (ECP)/i-TPU (solid electrolyte)/stainless-steel disc (electrode)). The UV–vis (400–800 nm) and UV–vis–NIR spectra (400–2400 nm) of the ECDs were recorded by using a UV–vis–NIR spectrometer (V-770, JASCO) with a resolution of 0.5 nm at a scan rate of 1000 nm min⁻¹.

Declaration of competing interest

The authors declare that they have no known competing financial interests or personal relationships that could have appeared to influence the work reported in this paper.

Acknowledgements

This work was supported by the Defense Acquisition Program Administration (DAPA) and Agency for Defense Development (ADD) under the contract UD170096GD, the Center for Advanced Soft Electronics under the Global Frontier Project (NRF-2014M3A6A5060932) and the Basic Science Research Program (2020R1A2C3014237 and 2017R1A5A1015596) of the National Research Foundation of Korea (NRF) funded by the Ministry of Science, ICT.

Appendix A. Supplementary data

Supplementary data to this article can be found online at <https://doi.org/10.1016/j.nanoen.2020.105199>.

References

- [1] R.T. Hanlon, Cephalopod dynamic camouflage, *Curr. Biol.* 17 (2007) R400–R404, <https://doi.org/10.1016/j.cub.2007.03.034>.
- [2] D.K. Oller, U. Griebel, G.B. Müller, T. Pradeu, K. Schäfer, *Evolution of Communication Systems: A Comparative Approach*, MIT Press, 2004.
- [3] C. Yu, Y. Li, X. Zhang, X. Huang, V. Malyarchuk, S. Wang, Y. Shi, L. Gao, Y. Su, Y. Zhang, Adaptive optoelectronic camouflage systems with designs inspired by cephalopod skins, *Proc. Natl. Acad. Sci. Unit. States Am.* 111 (2014) 12998–13003, <https://doi.org/10.1073/pnas.1410494111>.
- [4] L. Phan, R. Kautz, E.M. Leung, K.L. Naughton, Y. Van Dyke, A.A. Gorodetsky, Dynamic materials inspired by cephalopods, *Chem. Mater.* 28 (2016) 6804–6816, <https://doi.org/10.1021/acs.chemmater.6b01532>.
- [5] Q. Wang, G.R. Gossweiler, S.L. Craig, X. Zhao, Cephalopod-inspired design of electro-mechano-chemically responsive elastomers for on-demand fluorescent patterning, *Nat. Commun.* 5 (2014) 1–9, <https://doi.org/10.1021/acs.chemmater.6b01532>.
- [6] C. Larson, B. Peele, S. Li, S. Robinson, M. Totaro, L. Beccai, B. Mazzolai, R. Shepherd, Highly stretchable electroluminescent skin for optical signaling and tactile sensing, *Science* 351 (2016) 1071–1074, <https://doi.org/10.1126/science.aac5082>.
- [7] S. Li, B.N. Peele, C.M. Larson, H. Zhao, R.F. Shepherd, A stretchable multicolor display and touch interface using photopatterning and transfer printing, *Adv. Mater.* 28 (2016) 9770–9775, <https://doi.org/10.1002/adma.201603408>.
- [8] J. Liang, L. Li, X. Niu, Z. Yu, Q. Pei, Elastomeric polymer light-emitting devices and displays, *Nat. Photon.* 7 (2013) 817–824, <https://doi.org/10.1038/nphoton.2013.242>.
- [9] C. Grimsdale, K. Leok Chan, R.E. Martin, P.G. Jokisz, A.B. Holmes, Synthesis of light-emitting conjugated polymers for applications in electroluminescent devices, *Chem. Rev.* 109 (2009) 897–1091, <https://doi.org/10.1021/cr000013v>.
- [10] R.-P. Xu, Y.-Q. Li, J.-X. Tang, Side-chain engineering of green color electrochromic polymer materials: toward adaptive camouflage application, *J. Mater. Chem. C* 4 (2016) 9116–9142, <https://doi.org/10.1039/C6TC00197A>.
- [11] K. Lee, D.A. Davis, S.R. White, J.S. Moore, N.R. Sottos, P.V. Braun, Force-induced redistribution of a chemical equilibrium, *J. Am. Chem. Soc.* 132 (2010) 16107–16111, <https://doi.org/10.1021/ja106332g>.
- [12] C.-G. Granqvist, P. Lansäker, N. Milyuka, G. Niklasson, E. Avendano, Progress in chromogenics: new results for electrochromic and thermochromic materials and devices, *Sol. Energy Mater. Sol. Cells* 93 (2009) 2032–2039, <https://doi.org/10.1016/j.solmat.2009.02.026>.
- [13] G. Kim, S. Cho, K. Chang, W.S. Kim, H. Kang, S.P. Ryu, J. Myoung, J. Park, C. Park, W. Shim, Spatially pressure-mapped thermochromic interactive sensor, *Adv. Mater.* 29 (2017) 1606120, <https://doi.org/10.1002/adma.201606120>.
- [14] M. Irie, T. Fukaminato, K. Matsuda, S. Kobatake, Photochromism of diarylethene molecules and crystals: memories, switches, and actuators, *Chem. Rev.* 114 (2014) 12174–12277, <https://doi.org/10.1021/cr500249p>.
- [15] R.J. Mortimer, A.L. Dyer, J.R. Reynolds, Electrochromic organic and polymeric materials for display applications, *Displays* 27 (2006) 2–18, <https://doi.org/10.1016/j.displa.2005.03.003>.

- [16] P. Andersson, R. Forchheimer, P. Tehrani, M. Berggren, Printable all-organic electrochromic active-matrix displays, *Adv. Funct. Mater.* 17 (2007) 3074–3082, <https://doi.org/10.1002/adfm.200601241>.
- [17] E. Redel, J. Mlynarski, J. Moir, A. Jelle, C. Huai, S. Petrov, M.G. Helander, F. C. Peiris, G. von Freymann, G.A. Ozin, Electrochromic bragg mirror: ECBM, *Adv. Mater.* 24 (2012) OP265–OP269, <https://doi.org/10.1002/adma.201202484>.
- [18] J. Lee, L.G. Kaake, J.H. Cho, X.-Y. Zhu, T.P. Lodge, C.D. Frisbie, Ion gel-gated polymer thin-film transistors: operating mechanism and characterization of gate dielectric capacitance, switching speed, and stability, *J. Phys. Chem. C* 113 (2009) 8972–8981, <https://doi.org/10.1021/jp901426e>.
- [19] J. Yamamoto, Y. Furukawa, Electronic and vibrational spectra of positive polarons and bipolarons in regioregular poly (3-hexylthiophene) doped with ferric chloride, *J. Phys. Chem. B* 119 (2015) 4788–4794, <https://doi.org/10.1021/jp512654b>.
- [20] J.O. Guardado, A. Salleo, Structural effects of gating poly (3-hexylthiophene) through an ionic liquid, *Adv. Funct. Mater.* 27 (2017) 1701791, <https://doi.org/10.1002/adfm.201701791>.
- [21] D. Rawlings, E.M. Thomas, R.A. Segalman, M.L. Chabiny, Controlling the doping mechanism in poly (3-hexylthiophene) thin-film transistors with polymeric ionic liquid dielectrics, *Chem. Mater.* 31 (2019) 8820–8829, <https://doi.org/10.1021/acs.chemmater.9b02803>.
- [22] G.A. Niklasson, C.G. Granqvist, Electrochromics for smart windows: thin films of tungsten oxide and nickel oxide, and devices based on these, *J. Mater. Chem.* 17 (2007) 127–156, <https://doi.org/10.1039/B612174H>.
- [23] H.C. Moon, T.P. Lodge, C.D. Frisbie, Solution processable, electrochromic ion gels for sub-1 V, flexible displays on plastic, *Chem. Mater.* 27 (2015) 1420–1425, <https://doi.org/10.1021/acs.chemmater.5b00026>.
- [24] A.A. Argun, A. Cirpan, J.R. Reynolds, The first truly all-polymer electrochromic devices, *Adv. Mater.* 15 (2003) 1338–1341, <https://doi.org/10.1002/adma.200305038>.
- [25] P.M. Beaujuge, J.R. Reynolds, Color control in π -conjugated organic polymers for use in electrochromic devices, *Chem. Rev.* 110 (2010) 268–320, <https://doi.org/10.1021/cr900129a>.
- [26] P.M. Beaujuge, C.M. Amb, J.R. Reynolds, Spectral engineering in π -conjugated polymers with intramolecular donor–acceptor interactions, *Acc. Chem. Res.* 43 (2010) 1396–1407, <https://doi.org/10.1021/ar100043u>.
- [27] R.J. Mortimer, Electrochromic materials, *Annu. Rev. Mater. Res.* 41 (2011) 241–268, <https://doi.org/10.1039/C59972600147>.
- [28] H.-H. Chou, A. Nguyen, A. Chortos, J.W. To, C. Lu, J. Mei, T. Kurosawa, W.-G. Bae, J.B.-H. Tok, Z. Bao, A chameleon-inspired stretchable electronic skin with interactive colour changing controlled by tactile sensing, *Nat. Commun.* 6 (2015) 1–10, <https://doi.org/10.1038/ncomms9011>.
- [29] D.G. Seo, H.C. Moon, Mechanically robust, highly ionic conductive gels based on random copolymers for bending durable electrochemical devices, *Adv. Funct. Mater.* 28 (2018) 1706948, <https://doi.org/10.1002/adfm.201706948>.
- [30] D.F. Miranda, C. Versek, M.T. Tuominen, T.P. Russell, J.J. Watkins, Cross-linked block copolymer/ionic liquid self-assembled blends for polymer gel electrolytes with high ionic conductivity and mechanical strength, *Macromolecules* 46 (2013) 9313–9323, <https://doi.org/10.1021/ma401302r>.
- [31] A. Gonçalves, C. Costa, S. Pereira, N. Correia, M. Silva, P. Barbosa, L. Rodrigues, I. Henriques, R. Martins, E. Fortunato, Study of electrochromic devices with nanocomposites polymethacrylate hydroxyethylene resin based electrolyte, *Polym. Adv. Technol.* 23 (2012) 791–795, <https://doi.org/10.1002/pat.1966>.
- [32] M.T. Otley, M.A. Invernale, G.A. Sotzing, Fabric electrochromic displays for adaptive camouflage, biomimicry, wearable displays and fashion, *Electrochromic materials and devices*, Wiley-VCH Verlag GmbH & Co. KGaA, 2015, <https://doi.org/10.1002/9783527679850.ch16>.
- [33] A.L.-S. Eh, A.W.M. Tan, X. Cheng, S. Magdassi, P.S. Lee, Recent advances in flexible electrochromic devices: prerequisites, challenges, and prospects, *Energy Technol.* 6 (2018) 33–45, <https://doi.org/10.1002/ente.201700705>.
- [34] P.M. Beaujuge, S.V. Vasilyeva, S. Ellinger, T.D. McCarley, J.R. Reynolds, Unsaturated linkages in dioxthiophene–benzothiadiazole donor–acceptor electrochromic polymers: the key role of conformational freedom, *Macromolecules* 42 (2009) 3694–3706, <https://doi.org/10.1021/ma9002787>.
- [35] M.L. Jin, S. Park, Y. Lee, J.H. Lee, J. Chung, J.S. Kim, J.S. Kim, S.Y. Kim, E. Jee, D. W. Kim, An ultrasensitive, visco-poroelastic artificial mechanotransducer skin inspired by piezo2 protein in mammalian merkel cells, *Adv. Mater.* 29 (2017) 1605973, <https://doi.org/10.1002/adma.201605973>.
- [36] V.K. Thakur, G. Ding, J. Ma, P.S. Lee, X. Lu, Hybrid materials and polymer electrolytes for electrochromic device applications, *Adv. Mater.* 24 (2012) 4071–4096, <https://doi.org/10.1002/adma.201200213>.
- [37] C. Enengl, S. Enengl, S. Pluczyk, M. Havlicek, M. Lapkowski, H. Neugebauer, E. Ehrenfreund, Doping-Induced absorption bands in P3HT: polarons and bipolarons, *ChemPhysChem* 17 (2016) 3836–3844, <https://doi.org/10.1002/cphc.201600961>.
- [38] C.K. Chiang, C. Fincher Jr., Y.W. Park, A.J. Heeger, H. Shirakawa, E.J. Louis, S. C. Gau, A.G. MacDiarmid, Electrical conductivity in doped polyacetylene, *Phys. Rev. Lett.* 39 (1977) 1098, <https://doi.org/10.1103/PhysRevLett.39.1098>.
- [39] J.L. Bredas, G.B. Street, Polarons, bipolarons, and solitons in conducting polymers, *Acc. Chem. Res.* 18 (1985) 309–315, <https://doi.org/10.1021/ar00118a005>.
- [40] R.T. Hanlon, J.B. Messenger, *Cephalopod Behaviour*, Cambridge University Press, 1996.



Jehyoung Koo is a Researcher in Korea Institute of Industrial Technology (KITECH), South Korea. He received his M.S. degree in Chemical Engineering from Hanyang University, South Korea, in 2020, B.S. degree in Organic Materials and Fiber Engineering from Soongsil University, South Korea, in 2018. His current research interests focus on the polymer electrochromism based on ionic gel electrolyte and electronic skin



Dr. Vipin Amoli obtained his Ph.D. in Physics from Academy of Scientific & Innovative Research (AcSIR) India in 2016, M. Tech. in Nanotechnology from National Institute of Technology Kurukshetra in 2011, and M.S. in Physics from Hemvati Nandan Bahuguna Garhwal University in 2008. From 2016 to 2018, he worked as a postdoctoral fellow at Soongsil University (2016–2017) and Hanyang University (2017–2018), South Korea and then as a Research Assistant Professor (2019) at Hanyang University, South Korea. His research interests include electronic & ionic skins, soft actuators and flexible electrochromic devices.



Dr. So Young Kim is a Postdoctoral fellow in Korea Research Institute of Chemical Technology (KRICT), South Korea. She received her Ph. D. in the Department of Chemical Engineering from Hanyang University in 2019, M.S. in the Department of Organic Materials and Fiber Engineering from Soongsil University in 2014, and B.S. degree in the Department of Organic Materials and Fiber Engineering from Soongsil University in 2012. Her current research interests focus on sensors and transducer system based on hybrid organic/ionic materials.



Chaeyoung Lee received her B.S. degree from the Department of Physics at Hanyang University, South Korea, in 2019. She is currently a M.S. student in the Department of Chemical Engineering at Hanyang University, South Korea, under the supervision of Prof. Do Hwan Kim. Her research interests focus on the design and fabrication of electrochemical devices.



Junho Kim received his B.S. degree from the School of Electrical and Electronics Engineering at Chung-Ang University, South Korea, in 2018. He is currently a M.S./Ph.D. student in the School of Interdisciplinary Bioscience and Bioengineering at Pohang University of Science and Technology (POSTECH, Pohang, South Korea) under the supervision of Prof. Sung-Min Park. His main research interest is developing implantable medical device.



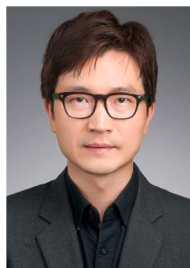
Sung-Min Park received the B.S. and Ph.D. degrees in electrical and computer engineering from Purdue University, West Lafayette, Indiana, U.S., in 2001 and 2006, respectively. He is currently a Professor of the department of Creative IT Engineering and Electrical Engineering at Pohang University of Science and Technology (POSTECH, Pohang, South Korea), where he has been with since 2016. From 2006 to 2014, he was with Medtronic (Minneapolis, Minnesota, U.S.) as R&D Manager, leading an award-winning team in developing the world first MRI conditional pacemaker. From 2014 to 2016, he was with Samsung (Suwon, South Korea) as Director, spearheading healthcare centric mobile device and mobile health service platform development projects. His current research interests include developing implantable medical device, artificial pancreas system, digital healthcare, and AI based closed loop algorithm.



Dr. Kyoung Jin Jung is a Principal Researcher at Agency for Defense Development (ADD), South Korea. He received his Ph. D. in Aerospace engineering from Korea Advanced Institute Science and Technology (KAIST) in 2010, and M.S. in Aerospace engineering from Seoul National University in 1992. From 1992 to present, he worked as a research engineer for ADD. His current research interests focus on electromagnetic materials design, aerodynamic and Radar Cross Section (RCS) analysis of aircraft.



Dr. Jeongsun Kim is a Principal Researcher at Agency for Defense Development (ADD), S. Korea from 1988 to present. He was in charge of the Nano Functional Materials Lab. in Defense Nano Technology Application Center (DNTAC) from 2008 to 2016. He received his Ph.D. in Materials Science Engineering from Korea Advanced Institute Science and Technology (KAIST) in 1998, and his M.S. degree at Hanyang University in 1988. Recently, his research interests are in the area of nanocomposites, electronic structure analysis, and intelligent materials.



Dr. Do Hwan Kim is currently a Professor in Department of Chemical Engineering at Hanyang University, South Korea. He received his Ph.D. in Chemical Engineering from Pohang University of Science and Technology in 2005. From 2006 to 2010, he worked at Samsung Advanced Institute of Technology as a senior researcher. Also, he worked at Stanford University, United States, as a postdoctoral fellow in Department of Chemical Engineering (2011–2012) and worked as an Assistant Professor at Department of Organic Materials and Fiber Engineering at Soongsil University, South Korea. (2012–2017). His research interests are in the field of organic optoelectronics, iontronic & electronic skins, and bioinspired sensor devices.



Dr. Joon Mo Ahn studied material engineering science at Yonsei University and obtained his Ph.D. at Yonsei University. From 1996, he has been worked at Agency for Defense Development (ADD), S. Korea, and from 2006 to 2007 he worked at Air Force Institute of Technology (AFIT), USA as an exchange scientist. His current research interests cover functional material science in electromagnetic field and infrared region, with a particular focus on energy absorbing and reflection materials.